Performance Analysis of a Dense Device to Device Network

Seung-Yeon Kim[1], Chi-Hun Lim[2] and Choong-Ho Cho[2]
[1] Department of Electronics and Information Engineering, Korea University
Sejong, Korea
[e-mail: kimsy8011@korea.ac.kr]
[2] Department of Computer and Information Science, Korea University
Sejong, Korea
[e-mail: crusade, chcho@korea.ac.kr]
*Corresponding author: Choong-Ho Cho

Received April 16, 2014; revised June 24, 2014; revised July 31, 2014; accepted August 17, 2014; published September 30, 2014

Abstract

Device-to-Device (D2D) communication is a technology component for long-term evolution-advanced (LTE-A). In D2D communication, users in close proximity to each other can communicate directly without going through a base station; such direct communication can improve spectral efficiency. Although D2D communication brings improvement in spectral efficiency, it also causes interference to the cellular network as a result of spectrum sharing. In particularly, D2D communication can generate interference for each D2D pair when the common wireless medium in a co-located limited area is accessed. Even though the interference management for between the D2D pair and cellular networks has been proposed, the interference reducing methods have still not been fully studied for the D2D pairs. In this paper, we investigate the problem of D2D pair coexistence in which interference is considered between D2D pairs. Using a signal to interference model for a target D2D pair, we provide an analysis of the aggregated throughput of a dense D2D network. For a target D2D pair, we assume that the desired signal and interference signals obey multipath fading and shadow fading. Through analysis, we demonstrate the effect of cluster size such as the number of D2D pairs and the size of the considered area on the network performance. The analytical results are compared with computer simulations. Our work can be used for a rough guideline for controlling the system throughput in a dense D2D network environment.

Keywords: Device to Device (D2D), cluster, co-located, operating condition, fading, performance evaluation

This work was supported by the Brain Korea 21 (BK 21) plus.

http://dx.doi.org/10.3837/tiis.2014.09.001

1. Introduction

Device-to-device (D2D) communication underlaying the cellular network has recently attracted a lot of attention in long-term evolution standardization. Transmission in a D2D pair occurs using one direct wireless link, whereas a conventional cellular uses two wireless links in which the base station (BS) is operated as the relay. Hence, by using D2D communication, the BS can be released from its function to forward data and thus improve spectral efficiency. The spectral efficiency is especially improved when multiple D2D links are able to operate simultaneously, using the same resources. The spectral efficiency is also improved by actively exploiting spatial diversity; devices in proximity of each other giving the opportunity to communicate directly and thus possibly to transmit their data with a lower signal power [1].

D2D use cases can be classified into peer-to-peer and relay types [2]. For the peer-to-peer case, D2D communications can be used to provide local data service when two geographically proximate users or devices want to exchange data, e.g., in the case of content sharing or context-aware applications. In relay cases, one of the communicating D2D devices has to relay the exchanged information to the BS which further forwards the data to the destination device.

Although D2D communication brings improvement in spectral efficiency and system capacity, since D2D communication occurs *under the umbrella* of a cellular network, in which D2D sessions take place in the same frequency band as the cellular communication, the interference caused by D2D links on the cellular communication must be contained. Additionally, D2D links also interfere with each other. Thus, interference management is one of the most critical issues for D2Ds underlaying cellular networks.

There are several devices which work to reduce the interference between D2D pairs and cellular networks. In [3], [4] and [5] restricting the transmit power schemes have been suggested to coordinate interference between D2D users and cellular users. Furthermore, a fixed booster factor and a back off factor have been proposed in [6] to dynamically control D2D power levels and limit D2D interference. In [7] and [8], authors proposed a resource allocation scheme in which a D2D link can reuse the resources for more than one cellular UE. In addition, a joint subcarrier and power allocation method using the spectrum sensing technique have been proposed in [9] to improve the spectrum efficiency.

Even though the interference management for between D2D pair and cellular networks was proposed, the interference reducing methods have still not been fully studied for between D2D pairs. Because of an absence of coordination between independent D2D pairs when accessing a wireless medium, devices will encounter high interference if several D2D pairs are simultaneously operating in crowded places, such as airports, international conferences, and shopping malls, where potential D2D users are located close to each other. Therefore, the study of interference gains importance because interference affects the throughput of a dense D2D network.

In order to illustrate this in detail, suppose that there are several D2D pairs that need to communicate privately within the same region, as shown in **Fig. 1**. In this scenario, because many D2D pairs exist densely, the pairs cause severe interference problems for D2D pair communication. The main contribution of this work is the derivation of an analytical model to obtain the maximum aggregated throughput of a dense D2D network deployed within the same region. In particular, this paper evaluates the outage probability and throughput by considering the modulation and coding scheme (MCS) based on the computation of the sum of

multiple small scale fading and large scale fading components. We use this analysis to develop system guidelines, and demonstrate the accuracy of the analytic model through a comparison with computer simulations.

The rest of this paper is organized as follows. Section 2 introduces the D2D pair network system model. The analytical model is presented in Section 3. In Section 4, numerical studies are discussed. Finally, concluding remarks are presented in Section 5.

2. System Model

Let us consider a limited circular region interference scenario that involves co-located D2D pairs. We assume that the interference between the cellular network and the D2D pair is managed efficiently using location-based, D2D mode selecting mechanisms [10]. Hence, we focus only on the interference caused by the coexistence of D2D pairs. In this scenario, D2D pairs are assumed to be uniformly distributed in a circular region of radius R from the target D2D receiver and organized in N D2D pairs with maximum radius D_R, as shown in **Fig. 1**.

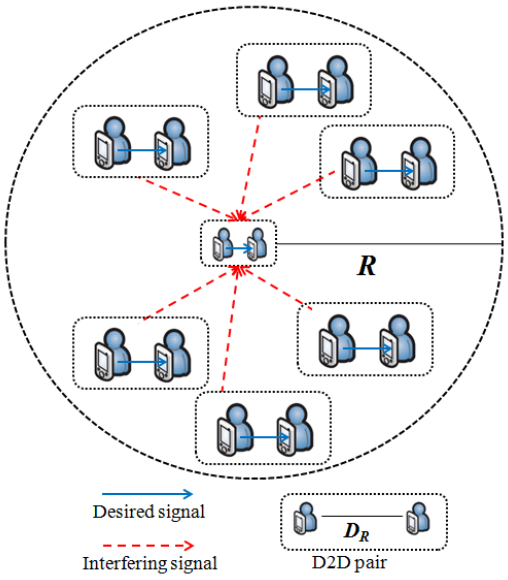

Fig. 1. System model of a dense D2D network.

To analyze the performance of a dense D2D network, we define the aggregated throughput of a dense D2D network, denoted by T_D, as

$$T_D = \sum_{i=1}^{N} T_D^i , \tag{1}$$

where T_D^i is the throughput of the D2D pair i conveyed to the D2D receiver in each of the N D2D pairs deployed in the region.

Let us assume that the most interfered D2D pair of our scenario is the central pair, given the assumption we made on the distribution of D2D pairs, where the most interfered D2D pair has

index 1. Therefore, we can define a lower bound on the aggregated throughput of a dense D2D network, T_{bound}, as

$$T_D \geq NT_D^1 = T_{bound}. \tag{2}$$

Under the considered scenario, the signal received at the target D2D receiver is

$$y = \sqrt{(u_M)^{-\alpha} P_D L_M} \cdot h_M \cdot s_M + \sum_{i=1}^{N-1} \sqrt{(u_I^i)^{-\alpha} P_D L_I^i} \cdot h_I^i \cdot s_I^i + n, \tag{3}$$

where s_M and s_I^i are the signals transmitted from the target D2D transmitter and from the interfering D2D transmitter i, respectively. u_M and u_I^i are the distance of the target D2D pair link and that of the target D2D receiver-interfering D2D transmitter i link, respectively, in a circular region. In Eq. (3), a path-loss model defined as $P_r = P_D \cdot (u_0)^{-\alpha}$ is used, where P_D and P_r denote the D2D transmit power and received signal power measured at u_0 away from the transmitter, respectively, and α is the path-loss exponent. Furthermore, L_M and L_I^i are a shadowing effect of the target D2D pair link and the target D2D receiver-interfering D2D transmitter i link, respectively, the natural logarithm of L_M and L_I^i is a Gaussian with a mean of zero and a standard deviation σ, where σ is $\sigma_{dB}(\ln 10)/10$. n is the additive white Gaussian noise (AWGN) at the receivers with power spectral density (PSD) N_0. In addition, h_M and h_I^i are the channel coefficient of the target D2D pair link and that of the target D2D receiver-interfering D2D transmitter i link; we assume that all channel coefficients follow a multipath fading that is fast, and the amplitude can be modeled by the Rician and Rayleigh distributions [11].

In the considered scenario, mostly there is a line-of-sight path for the desired signal of a target D2D pair communication. The fast component can then be modeled by a Rician distribution where the probability density function (PDF) is given by

$$f_{Rice}(x|p_{mp}) = \frac{x}{p'_{mp}} \exp\left(-\frac{x^2 + s_p^2}{2p'_{mp}}\right) I_0\left(\frac{xs_p}{p'_{mp}}\right), \quad 0 \leq x \leq \infty; \; s \geq 0$$

$$K = \frac{s_p^2}{2p'_{mp}}; \; p_{mp} = (K+1)p'_{mp}. \tag{4}$$

Here, x is the signal amplitude, p'_{mp} is the power of the scattered signal, s_p is the peak value of the directly received signal, $I_0(\cdot)$ is the modified *Bessel function* of the first kind and zeroth order [12], and K is the Rician factor, which depends on the ratio of the signal power from the dominant signal path relative to that of the scattered signal, and p_{mp} is the local mean power by path-loss and the shadowing effect. For Eq. (4), when a direct signal does not exist, i.e., s_p = 0 (K = 0 and $p_{mp} = p'_{mp}$), it become the Rayleigh distribution, where the PDF is given by

$$f_{Ray}(x|p_{mp}) = \frac{x}{p'_{mp}} \exp\left(-\frac{x^2}{2p'_{mp}}\right). \quad (5)$$

3. Analytical Modeling

In order to evaluate a lower bound on the aggregated throughput of a dense D2D network, let us focus our attention on the throughput of the target D2D pair, T_D^1, performed by the desired signal power of the target D2D pair, the sum of the interfering signals power of i interfering D2D transmitters in the same channel and the noise power as

$$T_D^1 = \left\{1 - \left[\sum_{i=1}^{N-1} \Pr[i] F(z_0|i)\right]\right\} \cdot M_L, \quad (6)$$

where $\Pr[i]$ is the probability that i interfering D2D pairs use the same channel that is assigned to the target D2D pair, $F(z_0|i)$ is the conditional probability that the desired signal power of the target D2D pair, P_d to the sum of the interfering signal powers by i interfering D2D transmitters, P_i and the noise power, P_n ratio is less than a predefined threshold value, z_0, as follows:

$$F(z_0|i) = \Pr\left[P_d / (P_i + P_n) < z_0|i\right]. \quad (7)$$

In general, -174dBm/Hz is used as the noise power spectral density for P_n. Thus, when this condition is considered in the system parameters, we approximate $P_i + P_n \approx P_i$ and then Eq. (7) can be expressed as

$$F(z_0|i) = \Pr\left[P_d / P_i < z_0|i\right] = \int_0^{z_0} dz \int_0^{\infty} f_{P_d}(zw) f_{P_i}(w) w dw. \quad (8)$$

In the last term of Eq. (6), M_L represents the bits per symbol according to the modulation and coding scheme (MCS) level, as a predefined threshold value, z_0.

In our study, for the desired signal, the Rician distribution as a multipath fading effect is considered. For the cases of an interfering signal, we consider the two cases in which the multipath fading effect is described by the Rician and Rayleigh distributions. In Eqs. (6) and (8), $\Pr[i]$ and $F(z_0|i)$ will be derived in the following sections. The performances of the analytic models considering Eq. (8) will be compared with the results of simulation considering the varying noise power spectral densities.

3.1 Modeling of Channel Interference Probability

As mentioned in the previous scenario, the analysis model consists of a target D2D pair and N-1 interfering D2D pairs. For given N-1 interfering D2D pairs, the probability of i D2D pairs using the same channel that is used by the target D2D pair, $\Pr[i]$, is approximated with N-1 independent Bernoulli trials as

$$\Pr[i]=\binom{N-1}{i}\cdot\rho^{i}\cdot(1-\rho)^{N-1-i}\ ,\quad i=0,1,2,\cdots,N-1. \tag{9}$$

Here, ρ is the probability that a co-channel is assigned to the target D2D pair and the interfering D2D pair.

3.2 Signal to Interference Ratio (SIR)

At first, let the signals of all D2D pairs obey the Rician fading effect. From Eq. (4), the PDF for the instantaneous desired signal power p of a target D2D pair is given by using $p = (1/2)x^2$

$$f_{p_d}(p|p_{od})=\frac{1}{p'_{mp}}\exp\left(-\frac{2p+s_p^2}{2p'_{mp}}\right)I_0\left(\frac{\sqrt{2p}s_p}{p'_{mp}}\right). \tag{10}$$

For the PDF of the sum of the interfering signal power of i interfering D2D pairs, we consider independent and identically distributed (i.i.d.) signals, each with the same Rician factor. Following the i time convolution of the Laplace transform method for Eq. (10) [13], we obtain

$$f_{P_i}(p|p_{od},i)=\frac{1}{2\cdot i\cdot p'_{I-mp}}\left(\frac{p}{i\cdot s_a^2}\right)^{(i-1)/2}\exp\left(-\frac{p+i\cdot s_a^2}{2\cdot i\cdot p'_{I-mp}}\right)I_{i-1}\left(\frac{\sqrt{p\cdot i\cdot s_a^2}}{i\cdot p'_{I-mp}}\right), \tag{11}$$

where s_a is the peak value of the directly received interfering signal a, and $I_{i\text{-}1}$ is the modified (i-1)th-order Bessel function of the first kind. From Eqs. (10) and (11), T_D^1 is derived in Appendix A as follows

$$T_D^1=M_L\cdot\sum_{i=1}^{N-1}\Pr[i]\left\{1-\frac{1}{\varepsilon_1^{i-1}}\times\exp\left(-\frac{\varepsilon_1^2}{2}\right)\times\int_0^{\infty}x^i\exp\left(-\frac{x^2}{2}\right)I_{i-1}[\varepsilon_1 x]Q\left[\beta,\sqrt{z_o\cdot\frac{i\cdot p'_{I-mp}}{p'_{mp}}}\cdot x\right]dx\right\}, \tag{12}$$

where $K_d=(p_{mp}/p'_{mp})-1$, $K_i=(p_{I-mp}/p'_{I-mp})-1$, $\varepsilon_1=\sqrt{2iK_i}$, $\beta=\sqrt{2K_d}$, and $Q(\cdot)$ is the Marcum Q function [11]. p_{mp} and p_{I-mp} can be obtained using the algorithm of Yeh and Schwartz [14].

Secondly, let the signal of a target D2D pair obey a Rician distribution and the interfering signal of interfering D2D pairs obey a Rayleigh distribution. When $K = 0$ for Eq. (11), the PDF of the sum of the interference signal powers by i interfering D2D pairs is given as

$$f_{P_i}(p|i)=\frac{1}{i\cdot p'_{I-mp}\,(i-1)!}\left(\frac{p}{i\cdot p'_{I-mp}}\right)^{i-1}\exp\left(-\frac{p}{i\cdot p'_{I-mp}}\right). \tag{13}$$

From Eqs. (10) and (13), we obtain the throughput T_D^1 for Eq. (6) as follows:

$$T_D^1 = M_L \cdot \left[1 - \sum_{i=1}^{N-1} \Pr[i] \left\{ 1 - \int_0^{\infty} \frac{t^{i-1}}{(i-1)!} \times \exp(-t) Q\left[\varepsilon, \sqrt{(2M_i t)}\right] dt \right\} \right], \quad (14)$$

where $\varepsilon \triangleq \sqrt{2K_d}$ and $M_i \triangleq z_0 \frac{i \cdot p'_{I-mp}}{p'_{mp}}$. Eq. (14) is derived in Appendix B.

Table 1. System Parameters

Parameters	Value
System Bandwidth	10MHz
D2D transmission power, P_D	10mW
D2D pairs radius, D_R	20m
Path loss exponent	4
Log-normal shadowing parameter in dB	4dB
Noise power spectral density	-174dBm/Hz

Table 2. MCS (modulation and coding scheme) level

MCS Level	**Modulation**	**Coding rate**	**SINR Threshold[*dB*]**	**Efficiency [*bits/symbol*]**
1	QPSK	1/12	-6.5	0.15
2	QPSK	1/6	-2.6	0.38
3	QPSK	1/2	1.0	0.88
4	16QAM	1/3	6.6	1.48
5	16QAM	3/5	11.4	2.41
6	64QAM	1/2	13.0	3.32
7	64QAM	3/4	15.6	4.52
8	64QAM	11/12	17.6	5.55

4. Numerical Studies

From the previous section, we obtained the analytic models of the two cases for the interfering D2D pair signals in which channel coefficients for interfering signal links, follow Rician fading and Rayleigh fading. In this section, we investigate the operating conditions of D2D pairs, such as a lower bound on the aggregated throughput of a dense D2D. The performances of the analytic models are compared with the simulation results by using the Monte Carlo simulation method. The system parameters for simulation and analysis are set as shown in **Table 1**. In addition, M_L according to z_0(= SINR) is shown in **Table 2** [15].

Fig. 2 shows the Rician factor K by path-loss and shadowing effect in which K is obtained by the local mean power p_{mp} and the scattered signal power p'_{mp} as shown in Eq. (4), for link of a main D2D pair. Based on the results shown in **Fig. 2**, it can be seen that if the distance between the transmitter and receiver of a target D2D pair increases, and/or p'_{mp} increases, then K is degraded.

Fig. 3 shows K by path-loss and shadowing effect in which K is obtained by the local mean power p_{mp} and the scattered signal power p'_{I-mp} as shown in Eq. (4), for the link of a target D2D receiver with i interfering D2D transmitters. As expected from previous results, if a

considered region from the receiver of a target D2D pair increases, and/or p'_{I-mp} decreases, K is degraded. We can also observe that as the number of interfering D2D pairs increases, K is decreased.

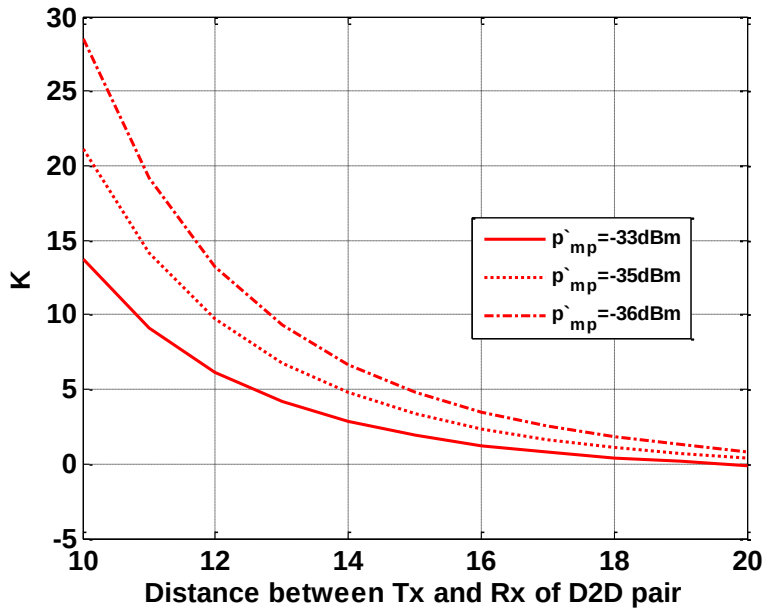

Fig. 2. Rician factor of a target D2D pair link versus D_R in varying p'_{mp} .

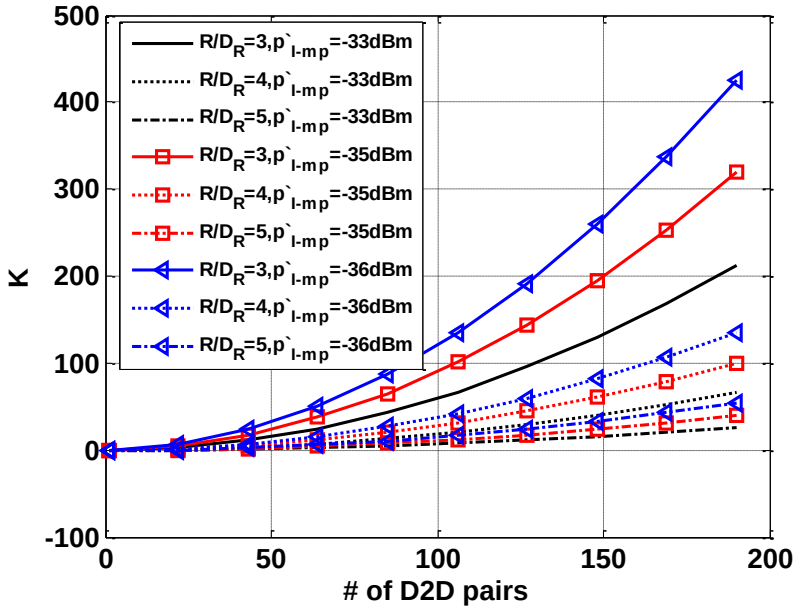

Fig. 3. Rician factor of a target D2D receiver with N interfering D2D transmitter links versus R with varying R/D_R and p'_{I-mp} .

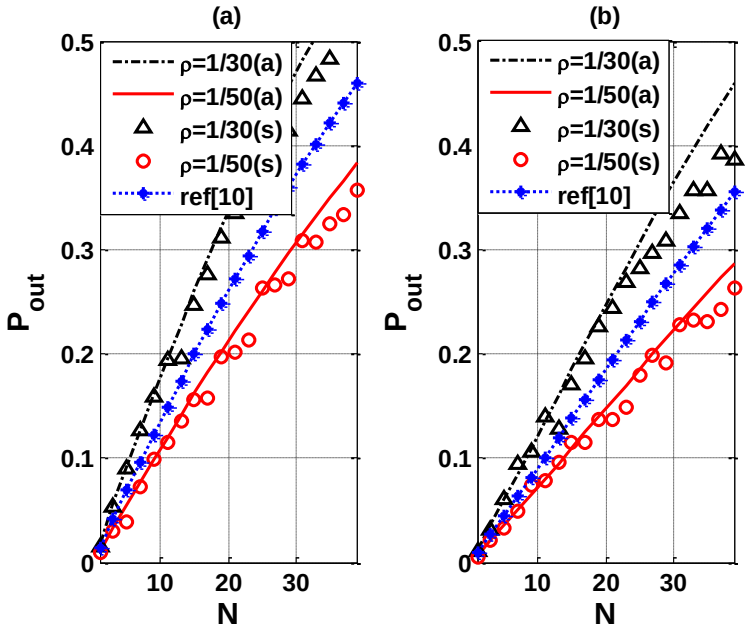

Fig. 4. Outage probability versus number of N interfering D2D pairs by varying ρ for (a) Rician fading and (b) Rayleigh fading, where z_0=1dB, K_d = 0.7, and $K_i = N \times K_d$.

In **Fig. 4**, the outage probabilities of the main D2D pair obtained by analysis and simulation for Rician fading (a) and Rayleigh fading (b) are shown. In this figure, we let R = 20m, and $p'_{mp} = p'_{I-mp} = -36\text{dBm}$. In addition, each outage probability is obtained from Eq. (8), when $z_0 <$ 1dB. We can observe that the results of the mathematical analysis agree reasonably well with those of the simulations. For an approximation of Eq. (8), we can see that the effect of the interference power is stronger than the noise power for the system performance, when the noise power spectral density is -174dBm/Hz, while this approximation is not suitable for the condition with the large noise power spectral density as shown in **Fig. 7** of Appendix C. We can also observe that as N and ρ increase, the outage probability increases. Lastly, when D2D pairs use the channel set fined by cognitive technique proposed in [9] is applied, we can see that ρ lies in between 1/50 and 1/30.

Fig. 5 describes the results of the outage probability and the aggregated throughput in Rician fading for the analytical model. In this figure, we use ρ = 1/50, which means that each D2D pair randomly selects only one channel among 50 channels in a long-term-evolution (LTE)-advanced cellular system with a 10 MHz channel bandwidth [16]. We also let M_L = 0.88 bits/symbol, and K = 0.7, according to z_0 = 1dB, respectively. From the figure, we can observe that the outage probability increases as N increases and R/D_R decreases. As expected from the results of the outage probability, the throughput increases as the ratio R/D_R increases. Through these results, we can obtain N = 49, 50, and 73, when R/D_R = 3, 4, and 5, respectively, to maximize T_{bound}.

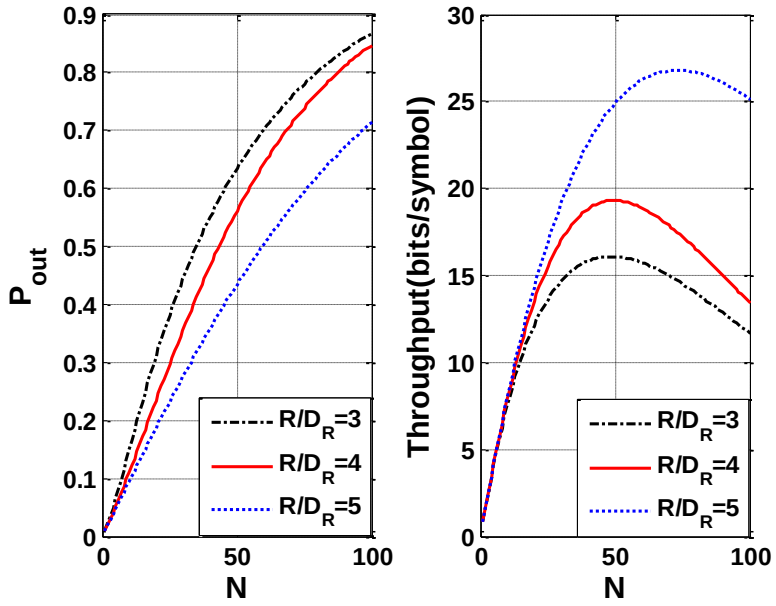

Fig. 5. Outage probability (left) and throughput (right) curves derived with the analytical model for varying N and R/D_R in Rician fading.

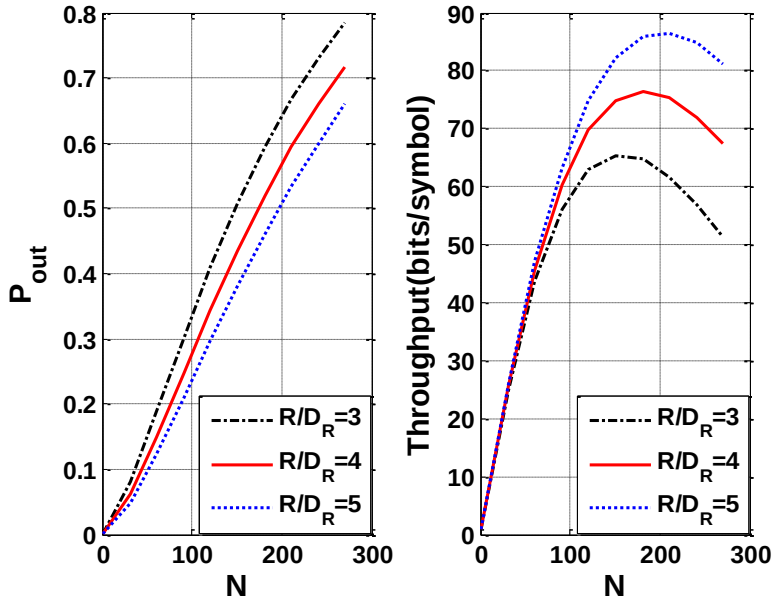

Fig. 6. Outage probability (left) and throughput (right) curves derived with the analytical model for varying N and R/D_R in Rayleigh fading.

Fig. 6 compares the outage probability and the aggregated throughput for different D2D cluster densities with Rayleigh fading in the analytical model. In this figure, we use $\rho = 1/50$, M = 0.88 bits/symbol, and K = 0.7. From the figure, both the outage probability and the

aggregated throughput have the same trend as in the previous figure for the increase of N and R/D_R. Through the results for the throughput, we can obtain N = 151, 181, and 211, when R/D_R = 3, 4, and 5, respectively, to maximize T_{bound}. As can be observed from the results in the graphs, variation in the density of D2D pairs has a significant impact on coexistence, especially when the density of D2D pairs becomes large.

5. Conclusion

In this paper, we introduce the problem of the coexistence of D2D pairs deployed in the same region. In addition, we derive an analytical model of the outage probability and aggregated throughput, considering propagation aspects with shadow fading and multipath fading effects. The majority of our analytical results show good agreement with the simulations in some conditions. The results show that the outage probability of a target D2D pair increases as the ratio R/D_R decreases, and the number of interfering D2D pairs increases, whereas the aggregated throughput of a dense D2D network increases as R/D_R decreases, and the number of interfering D2D pairs increases.

Appendix A

In order to obtain Eq. (12), we first derive $1-F\left(z_0|i\right)$ from Eq. (8) as follows:

$$1-F\left(z_0|i\right)=\int_{z_0}^{\infty}dz\int_{0}^{\infty}f_{pd}\left(zw\right)f_{pi}\left(w\right)wdw=\int_{0}^{\infty}f_{pi}\left(w\right)w\left(\int_{z_0}^{\infty}f_{pd}\left(zw\right)dz\right)dw. \tag{15}$$

In the second integration term of Eq. (15),

let $a=\int_{z_0}^{\infty}\frac{1}{2p'_{mp}}\exp\left(-\frac{zw+s_p^2}{2p'_{mp}}\right)I_0\left(\frac{\sqrt{zw}s_p}{p'_{mp}}\right)dz$, and $\sqrt{zw}=y$. That is

$$a=\int_{\sqrt{z_0w}}^{\infty}\frac{1}{2p'_{mp}}\exp\left(-\frac{y^2+s_p^2}{2p'_{mp}}\right)I_0\left(\frac{s_p}{p'_{mp}}y\right)\frac{2y}{w}dy\ . \tag{16}$$

Then, for Eq. (16), by letting $\frac{y}{\sqrt{p'_{mp}}}=x$, we obtain

$$a=\int_{\sqrt{\frac{z_0w}{p'_{mp}}}}^{\infty}\frac{1}{2p'_{mp}}\exp\left[-\frac{x^2+\left(\frac{s_p}{\sqrt{p'_{mp}}}\right)^2}{2}\right]I_0\left[\frac{s_p}{\sqrt{p'_{mp}}}x\right]\frac{2\sqrt{p'_{mp}}x}{w}\sqrt{p'_{mp}}dx$$

$$= \frac{1}{w} \int_{\sqrt{\frac{z_0 w}{p'_{mp}}}}^{\infty} \exp\left[-\frac{x^2 + \left(\frac{s_p}{\sqrt{p'_{mp}}} \right)^2}{2} \right] I_0\left[\frac{s_p}{\sqrt{p'_{mp}}} x \right] x dx$$

$$= \frac{1}{w} Q\left(\frac{s_p}{\sqrt{p'_{mp}}}, \sqrt{\frac{z_0 w}{p'_{mp}}} \right) = \frac{1}{w} Q\left(\beta, \sqrt{\frac{z_0 w}{p'_{mp}}} \right). \tag{17}$$

where $Q(a,b) = \int_b^{\infty} x \exp\left(-\frac{x^2 + a^2}{2} \right) I_0(ax) dx$.

Substituting Eq. (17) into Eq. (15),

$$1 - F(z_0|i) = \int_0^{\infty} f_{pi}(w) w \frac{1}{w} Q\left(\beta, \sqrt{\frac{z_0 w}{p'_{mp}}} \right) dw$$

$$= \int_0^{\infty} \frac{1}{2 \cdot i \cdot p'_{I-mp}} \left(\frac{w}{i \cdot s_p} \right)^{\frac{(i-1)}{2}} \exp\left(-\frac{w + i \cdot s_p}{2 \cdot i \cdot p'_{I-mp}} \right) I_{i-1}\left(\frac{\sqrt{i \cdot s_p \cdot w}}{i \cdot p'_{I-mp}} \right) Q\left(\beta, \sqrt{\frac{z_0 w}{p'_{mp}}} \right) dw. \tag{18}$$

In Eq. (18), let $\sqrt{\frac{i \cdot s_p}{i \cdot p'_{I-mp}}} = \varepsilon_1$, and $\sqrt{\frac{w}{i \cdot p'_{I-mp}}} = x$. That is:

$$1 - F(z_0|i) = \int_0^{\infty} \frac{1}{2 \cdot i \cdot p'_{I-mp}} \left(\frac{x}{\varepsilon_1} \right)^{i-1} \exp\left(-\frac{x^2}{2} \right) \exp\left(-\frac{{\varepsilon_1}^2}{2} \right) I_{i-1}(\varepsilon_1 x) \times Q\left(\beta, \sqrt{z_0 \frac{i \cdot p'_{I-mp}}{p'_{mp}}} x \right) \cdot i \cdot p'_{I-mp} (2x) dx. \tag{19}$$

Finally, we obtain

$$F(z_0|i) = 1 - \frac{1}{\varepsilon_1^{i-1}} \exp\left(-\frac{{\varepsilon_1}^2}{2} \right) \times \int_0^{\infty} x^i \exp\left(-\frac{x^2}{2} \right) I_{i-1}(\varepsilon_1 x) Q\left(\beta, \sqrt{z_0 \frac{i \cdot p'_{I-mp}}{p'_{mp}}} x \right) dx. \tag{20}$$

Appendix B

In order to obtain Eq. (14) from Eq. (20), let $b = \exp\left(-\frac{\varepsilon_1^2}{2}\right)\frac{1}{\varepsilon_1^{i-1}} I_{i-1}(\varepsilon_1 x)$.

Because $I_i(x) = \frac{1}{\Gamma(i+1)}\left(\frac{x}{2}\right)^i$ and $\Gamma(i) = (i-1)!$, b is rewritten as

$$b = \exp\left(-\frac{\varepsilon_1^2}{2}\right)\frac{1}{(i-1)!}\left(\frac{x}{2}\right)^{i-1}. \tag{21}$$

Substituting Eq. (21) into Eq. (20), for $\varepsilon_1 = 0$ by Ralyeigh fading, $F(z_0|i)$ is rewritten as

$$F(z_0|i) = 1 - \int_0^\infty x^i \exp\left(-\frac{x^2}{2}\right)\frac{1}{(i-1)!}\left(\frac{x}{2}\right)^{i-1} Q\left(\beta, \sqrt{z_0 \frac{i \cdot p'_{I-mp}}{p'_{mp}}}\, x\right) dx \,. \tag{22}$$

For Eq. (22), when $\frac{x^2}{2} = t$, $\sqrt{z_0 \frac{i \cdot p'_{I-mp}}{p'_{mp}}} = \sqrt{M_i}$, we obtain Eq. (14).

Appendix C

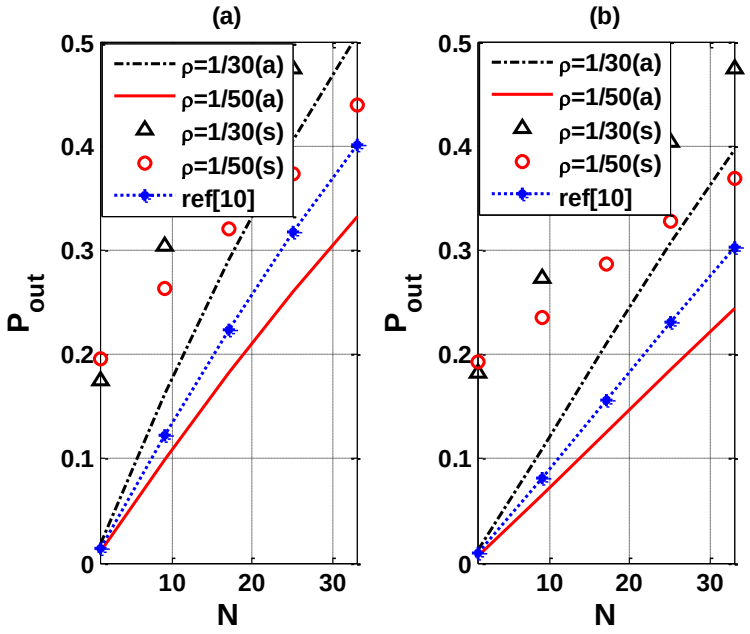

Fig. 7. Outage probability versus number of N interfering D2D pairs by varying ρ for (a) Rician fading and (b) Rayleigh fading, where z_0=1dB, K_d = 0.7, $K_i = N \times K_d$, and the noise power spectral density is -29dBm.

Fig. 7 shows the outage probabilities of the main D2D pair obtained by analysis and simulation for Rician fading (a) and Rayleigh fading (b) in R = 20m, $p'_{mp} = p'_{I-mp} = -36\text{dBm}$, and the noise power spectral density is -29dBm. In addition, each outage probability is obtained from Eq. (8), when $z_0 < 1$dB. We can observe that the results of the mathematical analysis do not agree with those of the simulations. It shows that in some conditions, in which the noise power spectral density is high, $P_i + P_n \approx P_i$ is not suitable.

References

[1] G. Fodor, E. Dahlman, G. Muldh, S. Parkvall, N. Reider, G. Miklo, and Z. Turanyi, "Design Aspects of Network Assisted Device-to-Device Communications," *IEEE Commun. Mag.*, vol. 50, no. 3, pp. 170-177, Mar. 2012. Article (CrossRef Link)

[2] L. Lei, Z. Zhong, C. Lin, and S. Shen, "Operator controlled device to device communications in LTE-advanced networks," *IEEE Wireless Mag*., vol. 19, no. 3, pp. 96-104, June 2012. Article (CrossRef Link)

[3] K. Doppler, M. Rinne, C. Wijting, C. Ribeiro, and K. Hugl, "Device-to-device communication as an underlay to LTE-advanced networks," *IEEE Commun. Mag*., vol. 47, no. 12, pp. 42-49, Dec. 2009. Article (CrossRef Link)

[4] B. Kaufman and B. Aazhang, "Cellular networks with an overlaid device to device network," in *Proc. of IEEE Asilomar Conf. on Signals, Syst. and Comput*., pp. 1537-1541. 2008. Article (CrossRef Link)

[5] M. C. Erturk et al., "Distributions of Transmit Power and SINR in Device-to-Device Networks," *IEEE Comm. Letts*., vol. 17, no. 2, pp. 273-276, Jan. 2013. Article (CrossRef Link)

[6] P. J¨anis, C. Yu, K. Doppler, C. Ribeiro, C. Wijting, K. Hugl, O. Tirkkonen, and V. Koivunen, "Device-to-device communication underlaying cellular communications systems," *Int'l J. of Commun., Network and Syst. Sci.*, vol. 2, no. 3, pp. 169-178, 2009. Article (CrossRef Link)

[7] H. Min, J. Lee, S. Park, and D. Hong, "Capacity enhancement using an interference limited area for device-to-device uplink underlaying cellular networks," *IEEE Trans. Wireless Commun.*, vol. 10, no. 12, pp. 3995- 4000, Dec. 2011. Article (CrossRef Link)

[8] Z. Wang, H. Tian, K. Yang and Z. Liu, "Frequency resource allocation strategy with QoS support in hybrid cellular and Device-to-Device networks," *Int. J. Communi. Syst*., vol. 9, no. 2, pp. 495-500, Feb. 2014. Article (CrossRef Link)

[9] Chen, Yueyun, Xiangyun Xu, and Qun Lei. "Joint Subcarriers and Power Allocation with Imperfect Spectrum Sensing for Cognitive D2D Wireless Multicast." *KSII Trans. Internet and Information Syst.*, vol. 7, no. 7, pp. 1533-1546, Jul. 2013. Article (CrossRef Link)

[10] Min, H., Seo, W., Lee, J., Park, S., and Hong, D., "Reliability improvement using receive mode selection in the device-to-device uplink period underlaying cellular networks," *IEEE Trans. Wirel. Commun.*, vol. 10, no. 2, pp. 413-418. Feb., 2011. Article (CrossRef Link)

[11] J. G. Proakis, Digital Communications, 2nd ed. McGraw-Hill, New York, 1989.

[12] N.W. McLachlan, *Bessel Functions for Engineers*. Oxford, U.K.: Oxford Univ. Press., 1955.

[13] M. Abramowitz and I. A. Stegun, *handbook of Mathematical functions*. New York: Dover, 1964, ch.9 and 29.

[14] Abu-Dayya and N. C. Beaulieu, "Outage probabilities in the presence of correlated lognormal interferers," *IEEE Trans. Veh. Technol*., vol. 43, no. 1, pp. 164-173, Feb. 1994. Article (CrossRef Link)

[15] D. L.-P, A. L, A. J, H. R, and J.Z, "Optimization Method for the Joint Allocation of Modulation Schemes, Coding Rates, Resource Blocks and Power in Self-Organizing LTE Networks," in *Proc. of IEEE INFOCOM*, Shanghai, China, April 2011. Article (CrossRef Link)

[16] I. F. Akyildiz, D. M. Gutierrez-Estevez and E.C. Reyes, *The Evolution to 4G Cellular Systems: LTE-Advanced*, Elesevier: Physical Comm., 2010.

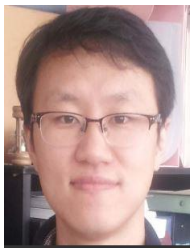

Seung-Yeon Kim received the Ph.D. degree in electronics and information engineering in 2012 from Korea University, Korea. He is currently a research professor in the Department of electronics and information engineering. He has participated in various research projects involving an IMT‐Advanced system, cognitive radio, and interference management. His research interests include performance evaluation of communication networks.

Chi‐Hun Lim received the Ph.D. degree in the Laboratory for Data Communication and Networks, Korea University. He has participated in various research projects involving an IMT‐Advanced system, security techniques for smart car. He is interested in handover protocols, resource management, and design and analysis of the next generation wireless communication systems.

Choong-Ho Cho received B.S. and M.S. degrees in industrial engineering from Korea University in 1981 and 1983, respectively. He received M.S. and Ph.D. degrees in computer science from the Institute National des Sciences Appliques, Lyon, France, in 1986 and 1989, respectively. He was an assistant professor at Sooncheunhyang University from 1990 to 1994, and is currently a professor at Korea University. He was a visiting professor at university of Washington from 2001 to 2002. His research interests include IT convergence technology, Building Energy Management System, 4G/5G mobile/wireless networks, D2D communication, small cell and SDN.